

Subgrain growth in Al and Al-1% Mn during annealing

ROLF SANDSTRÖM, BÖRJE LEHTINEN, EMMY HEDMAN,
IOANA GROZA, SONJA KARLSSON

Swedish Institute for Metals Research, Drottning Kristinas väg 48, S-114 28 Stockholm, Sweden

The subgrain growth during annealing of cold-worked Al-1% Mn and Al(4N) has been measured in the temperature intervals 300 to 400° C and 100 to 200° C respectively. For Al-1% Mn the subgrain diameter showed a parabolic growth, while for Al the diameter gradually reached a constant value. The microstructural investigations which included *in situ* annealing in a high voltage electron microscope demonstrated that the operating mechanism for growth in the higher temperature range was collective migration of sub-boundary dislocations. In the lower temperature range extraction of dislocations was found to be the dominating mechanism, i.e. dislocations partly lying in the boundaries are pulled out by the stress field in the subgrain interior. The observed growth rates were consistent with models for these mechanisms presented in two previous papers.

1. Introduction

During the annealing of cold-worked materials polygonalization occurs, in particular in alloys with a high stacking fault energy, resulting in the formation of subgrains. The size of the subgrains depends on the degree of reduction during cold-working, annealing temperature, and annealing time.

Subgrain growth can occur in two distinct ways: by the migration of sub-boundaries, and through subgrain coalescence. The migration of sub-boundaries results in growth which has much in common with conventional grain growth. The boundaries migrate in such a way that the large subgrains grow at the expense of small ones. This process has been discussed in detail, and a model for its contribution to the growth rate has been derived in [1]. Three mechanisms for subgrain coalescence by the dissolution of sub-boundaries were presented in [2]: collective migration, extraction, and emission of boundary dislocations. Expressions for their contributions to the growth rate were also given.

Collective migration involves the simultaneous movement of the dislocations in a sub-boundary. If this movement occurs in the boundary plane in

such a way that the average distance between the dislocations increases, it can lead to the dissolution of the boundary. This mechanism for subgrain coalescence was proposed by Li [3]. On the other hand, if the movement takes place in another direction the whole boundary will migrate, which can give rise to subgrain growth as pointed out above. Extraction means that a dislocation which is only partly lying in a boundary is pulled out by the stress field in the subgrain interior. This should be contrasted to the emission of a dislocation which is situated entirely in the boundary.

The purpose of the present paper is to analyse the operating mechanisms for subgrain growth in Al-1% Mn and Al. Measurements are presented for the variation of the subgrain size during annealing. These measurements are compared to models for subgrain growth.

2. Experimental

2.1. Materials

Two materials were used in this investigation: Al-1% Mn and pure Al. The analysis of Al-1% Mn alloy was 1.10 Mn, 0.06 Fe and 0.01 Si (wt %), the remainder being Al. The aluminium material was of 4N purity, the main impurity being silicon.

The Al-1% Mn alloy was prepared in the following way. The 37 mm thick ingot was cold-worked to 10 mm, solution treated at 640°C for 4 h, air cooled, cold-rolled to 2 mm, annealed at 500°C for 10 min and quenched to obtain a grain size of 130 μm , and finally cold-rolled again to 80% reduction in thickness. The strips thus obtained were annealed for various times (5, 30, 60 and 120 min) at 300, 350, 400°C. The cast pure Al material was cold-rolled from 27 mm to 2 mm, annealed in a salt bath for 10 sec at 400°C, quenched to obtain a grain size of 110 μm , and finally cold-rolled to 80% reduction. To study subgrain growth the material was then annealed for 5, 30, 60 and 120 min at 100, 150 and 200°C.

2.2. Subgrain diameter measurements

The measurements were made both in a 100 kV (Philips 300) and a 1000 kV (JEOL 1000D) electron microscope to take advantage of the high specimen tilting angles in the former and the higher penetration of the latter. The subgrain size was determined by a linear intercept analysis on the transmission electron micrographs. For the subgrain size measurements, 8 to 10 pictures were taken of the same area with different foil orientations so as to have different subgrains in contrast successively. When a polygonized structure is developed, the sub-boundaries comprise regular dislocation networks separating misoriented regions, and so if a clear sub-boundary was not observed, neighbouring subgrains could be distinguished by a difference in contrast. A network where the distance between the dislocations was larger than 100 nm was not considered to be a sub-boundary. This corresponds to the lower limit of misorientation between the subgrains of 0.1 to 0.2°. No distinction has been made regarding the degree of perfection of a network. Thus after short annealing times at low temperatures there are still boundaries of considerable "cell wall" character surrounded by dislocation tangles. These boundaries have been taken into account when measuring the subgrain size. For subgrain size data obtained from 1000 kV micrographs the apparent diameter has been corrected for overlapping of subgrains because of the thicker specimens used.

3. Growth in Al-1% Mn

Subgrain growth during annealing of cold-rolled Al-1% Mn has been observed at 300, 350 and 1230

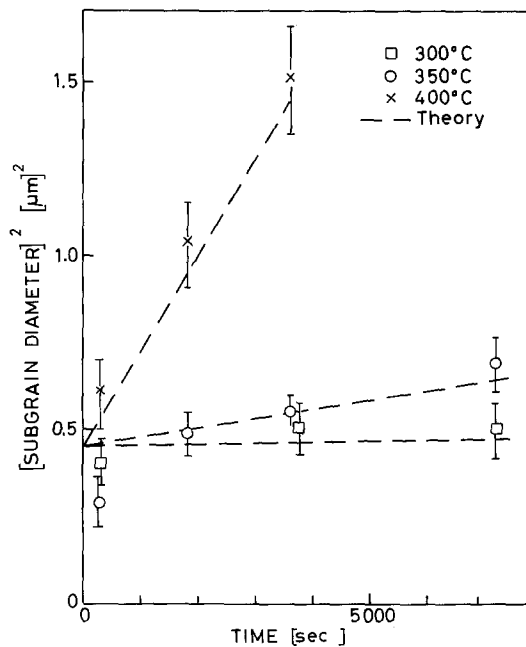


Figure 1 Subgrain diameter squared versus annealing time at 300, 350 and 400°C for 80% cold-rolled Al-1% Mn.

400°C. The results are presented in Fig. 1. As can be seen, the subgrain growth is small at 300 and 350°C. The growth rate is essentially greater at 400°C, but the total range of subgrain diameters observed is still rather limited. It was not possible to proceed to longer times at 400°C because the specimens were then completely recrystallized.

The substructure during annealing is illustrated in Fig. 2. The sequence shows specimens which have been heat treated for 5, 30, 60 and 120 min at 350°C. The substructure does not change very markedly in this sequence. The density of dislocations in the subgrain interiors is low. It is perhaps slightly higher for the shorter annealing times, but most subgrains are almost free of dislocations even for these annealing times. Since all micrographs have been taken under a number of different diffraction conditions, it has been possible to check that the low dislocation density is not an artifact due to dislocations being out of contrast. The low dislocation density is quite significant. It implies that extraction or emission of dislocations from the boundaries gives a negligible contribution to the growth rate. Out of the four mechanisms proposed for subgrain growth only two remain: boundary migration growth and growth by migration in the boundaries. It is obvious that boundary migration occurs. A great number of sub-boundaries are smoothly curved in

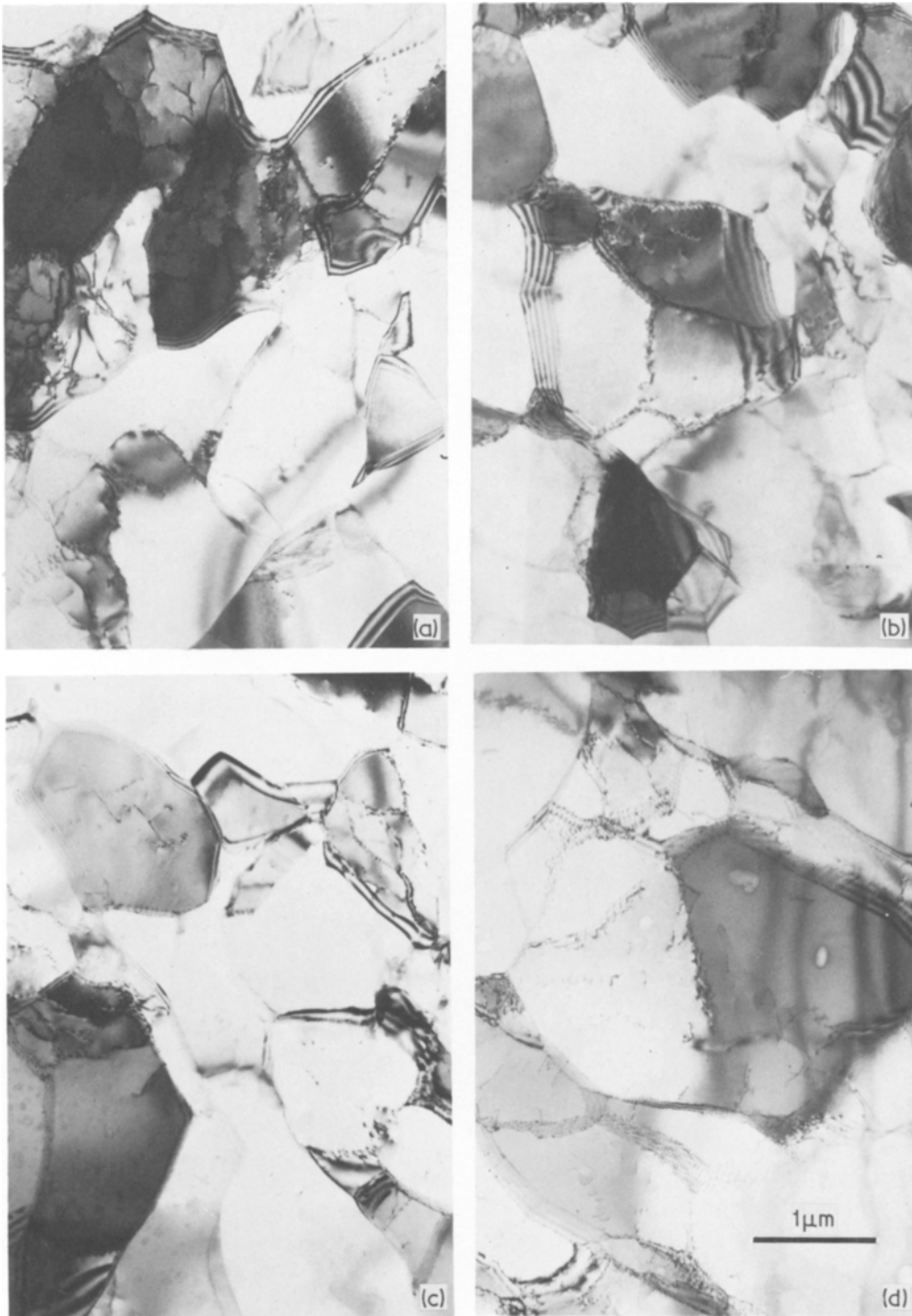


Figure 2 Development of the substructure in Al-1% Mn during annealing. Quenched after (a) 5, (b) 30, (c) 60, and (d) 120 min at 350° C.

Fig. 2 which indicates that the boundaries have been migrating before the specimen was quenched. Boundary migration requires that migration of dislocations in the boundaries takes place. To what

extent the migration in the boundaries gives rise to dissolution of sub-boundaries cannot be judged from static experiments.

To study the operating mechanisms during

growth further, *in situ* experiments have been performed in the high voltage electron microscope. Specimens were heated inside the microscope and observed during annealing. It must at once be realized that subgrain grain growth in thin foils and in bulk material are not entirely equivalent. Growth in thin foils is affected by the presence of the foil surfaces and is unavoidably two-dimensional to a certain extent, and this will of course affect the driving force. Although the growth is influenced by the presence of the foil surfaces and thermal stresses, it is still believed that valuable insight into the operating mechanisms can be obtained from *in situ* experiments. Some of the results of this investigation on Al-1% Mn have been reported previously [4]. A sequence of micrographs is presented there which shows how a small subgrain is consumed by its larger neighbours. This occurs in much the same way as conventional grain growth, and gives evidence for the occurrence of subgrain growth by boundary migration. Boundary dissolution has also been observed *in situ*. This is also illustrated in [4]. A boundary is emitting one dislocation after another until the boundary is completely dissolved. After having left the boundary the dislocations are gliding away to other sub-boundaries.

It is evident from Fig. 1 that the subgrain diameter D satisfied a parabolic growth law

$$D^2 = D_0^2 + Kt, \quad (1)$$

where D_0 is the initial subgrain size, t the time and K a temperature dependent constant. Such a time dependence is predicted both for growth by boundary migration [1] and by dislocation migration in the boundaries [3]. The constant K takes the following values in the respective cases;

$$K_{BM} = 3 M \tau_s \quad (2)$$

$$K_{MDB} = 8 M \tau_s \quad (3)$$

where M is the dislocation mobility for climb, and τ_s is the line tension of the dislocations in the sub-boundaries. These two contributions to the subgrain growth thus have identical form apart from the numerical factor. The theory therefore predicts that the two contributions will always appear simultaneously. It is very difficult to imagine that the boundary dislocations would be able to migrate in one direction but not in another, and it is thus physically quite reasonable that the two mechanisms appear together [2]. For the

numerical comparison between experiment and theory Equations 2 and 3 can be added

$$K = 11 M \tau_s. \quad (4)$$

This expression is independent of the sub-boundary angle, i.e. the misfit angle between adjacent subgrains. The line tension τ_s has been estimated as $Gb^2/3.5$ [1] where G is the shear modulus and b the Burgers vector. The mobility M for a pure element is given by [5],

$$M_0 = \frac{D_s b}{kT}, \quad (5)$$

where D_s is the coefficient for self diffusion, and kT has its usual meaning. For a solid solution an additional factor appears [1]

$$\frac{M}{M_0} = \frac{\ln(R_d/r_0)}{\ln(R_d/r_1) + D_v[1/D^A + 1/D^B \exp(-\Delta E/kT)] \ln(r_1/r_0)} \quad (6)$$

The quantities in Equation 6 have the following meanings. R_d is the conventional cut-off radius for the stress fields from dislocations which is of the order of the distance between dislocations in the subgrain interior. R_d is put equal to 10^{-7} m, $r_1 \approx 3b$ is the radius of the near core region, where the diffusion is appreciably affected by the rearrangement of atoms around a dislocation. $r_0 \approx b$ is the core radius. ΔE is the interaction energy between the solute atoms and the dislocation core. D_v is the diffusion coefficient for the alloy, D^A and D^B the diffusion coefficients for solvent and solute atoms respectively. For D_v and D^A values for pure aluminium have been used: $D_v = D^A = D_{Al} = D_{Al}^0 \exp(-Q_{Al}/kT)$ where $D_{Al}^0 = 10^{-5} \text{ m}^2 \text{ sec}^{-1}$ and $Q_{Al} = 128 \text{ kJ}$ [6]. These coefficients are normalized as self-diffusion coefficients and consequently D_s takes the same values. For D^B which describes the diffusion of Mn atoms in the alloy, $D_{Mn}^0 = 2.2 \times 10^{-5} \text{ m}^2 \text{ sec}^{-1}$ and $Q_{Mn} = 120 \text{ kJ mol}^{-1}$ have been chosen [6].

The theoretical results are included in Fig. 1. It is difficult to obtain an accurate value for the interaction energy ΔE . The value used in Fig. 1 which gives the best fit is $\Delta E = 59 \text{ kJ mol}^{-1}$. It is evident that the interaction energy obtained in this way leads to an activation energy for the whole process which is in good agreement with the experimental results, since the temperature

dependence of the growth rate is satisfactorily described. With the aid of linear elasticity theory it is possible to estimate ΔE and check whether the value found above is of the correct order of magnitude. The following expression is obtained [7]

$$\Delta E = -4G r_a^3 \eta_a, \quad (7)$$

where r_a is the atomic radius and η_a a misfit parameter. η_a is related to the linear lattice expansion δ_1 due to a volume fraction f of solute atoms

$$\eta_a = \frac{\delta_1}{f}$$

For Al-1% Mn, δ_1 is not entirely linear in f . About 0.4 wt % Mn is expected to be in solid solution after the heat treatment utilized. This yields a value for η_a of -0.167 if Hoffmann's results [8] for δ_1 are used. Inserting this value into Equation 7 gives $\Delta E = 41 \text{ kJ mol}^{-1}$ (0.43 eV). Linear elasticity cannot be expected to give a very accurate value for the interaction energy ΔE , since the strains in the core region are highly nonlinear. Thus the two ΔE values must be considered to be reasonably close. It can be concluded that the theoretical result is consistent with the sub-grain growth rates observed for Al-1% Mn.

4. Growth in aluminium

Subgrain growth has been studied at 100, 150, and 200°C in pure aluminium cold-rolled to 80% reduction. The subgrain diameters measured as a function of annealing time are presented in Fig. 3. The annealing times have been scaled to 150°C according to a procedure which will be described below. This simplifies the comparison with theory.

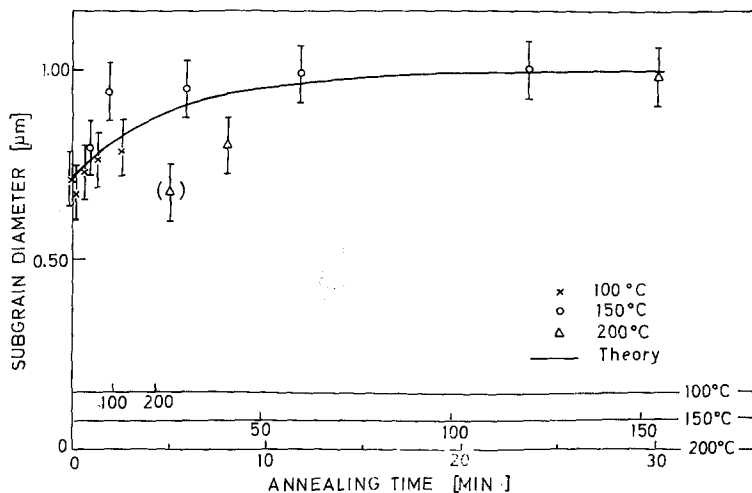


Figure 3 Subgrain diameter versus annealing time at 100, 150, and 200°C for 80% cold-rolled aluminium. To confirm the theoretical results different time scales have been used at the different temperatures. The scaling corresponds to an activation energy of 56 kJ mol^{-1} .

The data in Fig. 3 are consistent with a growth for which the subgrain size reaches a temperature independent asymptotic limit.

In Fig. 4 the development of the substructure during annealing at 150°C is illustrated. The substructure before annealing is also included. It is evident from Fig. 4a that sub-boundaries have already been formed during cold-rolling. Thus there are narrow and sharp boundaries. In micrographs at higher magnification the internal structure can be seen. This consists of fairly regularly ordered parallel dislocations with a spacing of 10 to 100 nm. During annealing the internal structure of the sub-boundaries is gradually getting more perfect as is apparent from Fig. 4. This is even more obvious at 200°C.

From Fig. 4 it is evident that the dislocation density in the subgrain interior is decreasing during annealing. This comparison is possible to make, because the micrographs have been taken for foil thicknesses of the same order of magnitude. This decrease has also been observed at 100 and 200°C. After the longest annealing times at 150 and 200°C the subgrains interiors are fairly free from dislocations.

In the cold-rolled condition and after the shortest annealing times there are still quite a few dislocation tangles, reminiscent of cell boundaries. However, the tangles gradually disappear during annealing and after the longest annealing times at 150 and 200°C practically no tangles remain.

A qualitative change of the substructure occurs during the heat treatment. The internal structure of the sub-boundaries becomes more perfect, the dislocations in the boundaries are ordered and the

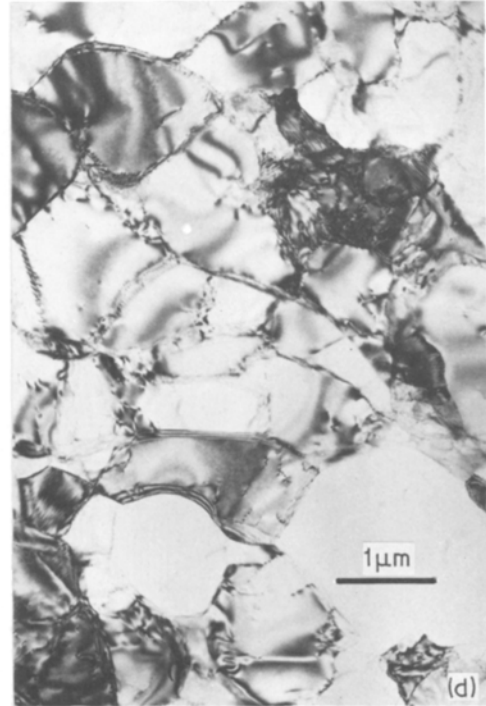


Figure 4 Development of the substructure in aluminium during annealing at 150° C. (a) Before annealing; (b), (c), (d) quenched after 5, 30, and 120 min respectively at temperature.

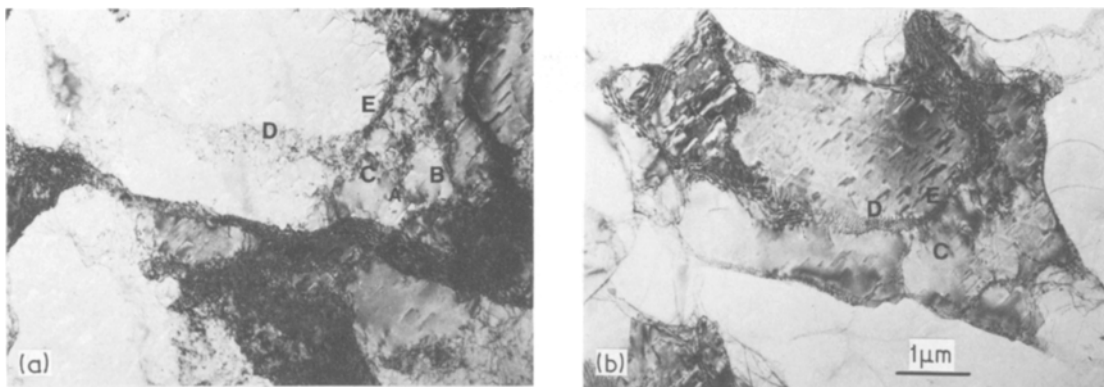


Figure 5 Specimen (a) before and (b) after annealing in the high voltage electron microscope. The micrographs demonstrate subgrain coalescence without boundary migration occurring simultaneously. Thus the boundaries marked A and B have disappeared in (b) and so almost has C. During the annealing the dislocation network in boundaries such as D and E has become more ordered.

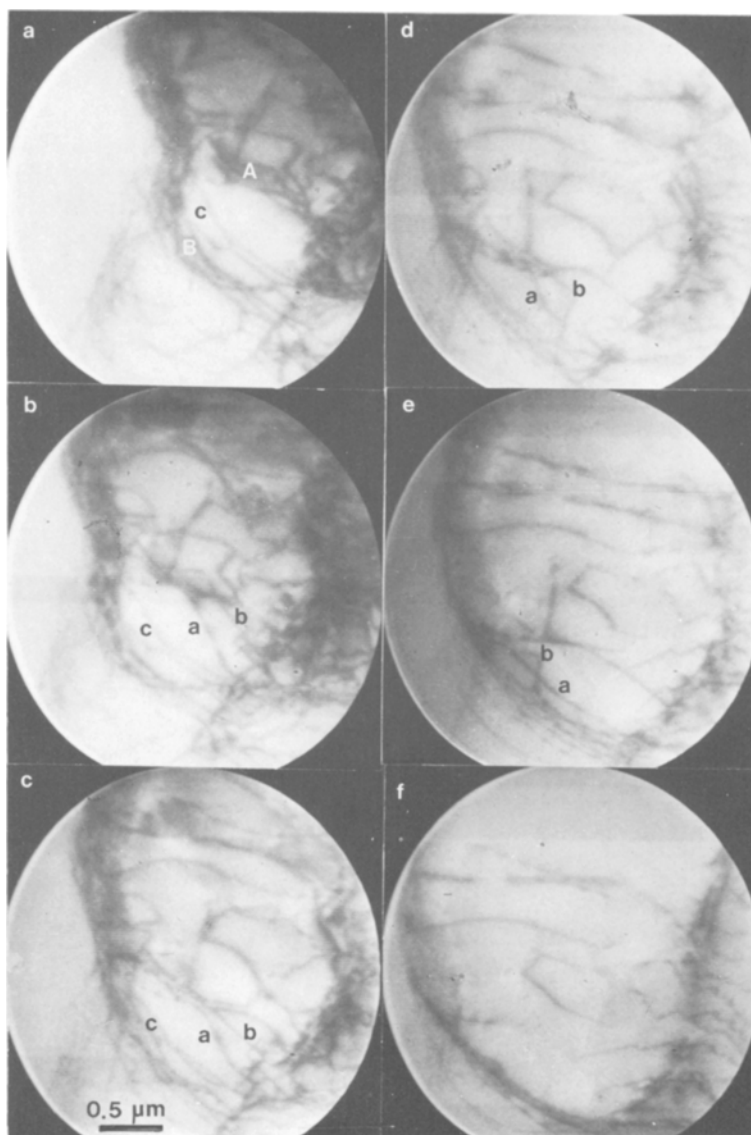


Figure 6 The sequence shows the dissolution of a boundary marked A. This occurs by the extraction of boundary dislocations like “a” and “b”. These two dislocations are finally absorbed by the boundary B. Simultaneously with the dissolution of A a gradual decrease in the dislocation density in the subgrain interiors takes place by annihilation and by absorption at the boundaries. The latter process is illustrated by the two dislocations marked “c” which are absorbed at the boundary B.

tangles disappear. At the same time the dislocation density in the subgrain interior is decreasing. These observations should be contrasted with those for Al-1% Mn at higher temperatures, where although a quantitative change of the subgrain size took place, no qualitative modification of the substructure was seen. Compared to the Al-1% Mn case there is another significant difference as well. In Fig. 2 the sub-boundaries are curved, indicating that they were migrating before the specimens were quenched. In Fig. 4 there is little or no sign of migrating boundaries. Thus, out of the four mechanisms proposed in [1] and [2] for subgrain growth, either extraction or emission of boundary dislocations is likely to yield the dominating contribution. Growth by dislocation migration in the boundaries can be excluded, since it always appears together with boundary migration according to arguments given in the previous section. The probability for the emission of dislocations is quite low except in the initial stage of recovery [2]. Since some recovery has occurred already during the cold working the contribution from emission of dislocations can be expected to be small. In summary, the micrographs together with analytical estimates, suggest that the subgrain growth occurs by the extraction of dislocations.

To substantiate these conclusions, further specimens have been annealed in the high voltage electron microscope. An example is shown in Fig. 5. The same area of a cold-rolled specimen is seen before and after annealing. The annealing temperature is of the order of 150° C. Comparing Figs. 5a and b one finds that no boundaries have been migrating. However, some boundaries have disappeared in Fig. 5b, thus contributing to the growth through subgrain coalescence, for example the boundaries marked A and B in Fig. 5a. Some boundaries like C have almost vanished. During the annealing the nature of a number of boundaries has changed. For example, D and E are surrounded by dislocation tangles in Fig. 5a, but these have disappeared to a large extent in Fig. 5b, and ordered dislocation networks are clearly seen. This is particularly apparent for the boundary D.

The dissolution of a boundary is shown in Fig. 6, which is taken from the video-tape recorded during annealing in the high voltage electron microscope. The boundary in question is marked A. The ordering of the dislocations in the boundary A is not completed before the dissolution starts. The dissolution occurs by the extraction of dislocations from the boundary. Examples are the dislocations "a" and "b". It can be seen that these

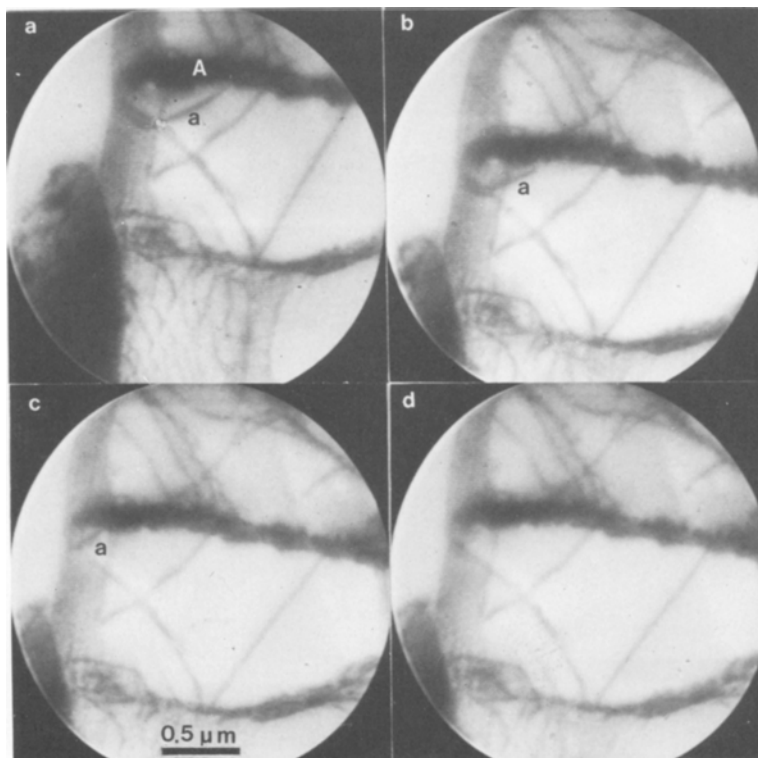


Figure 7 Extraction of a dislocation (marked "a") from a boundary (marked A).

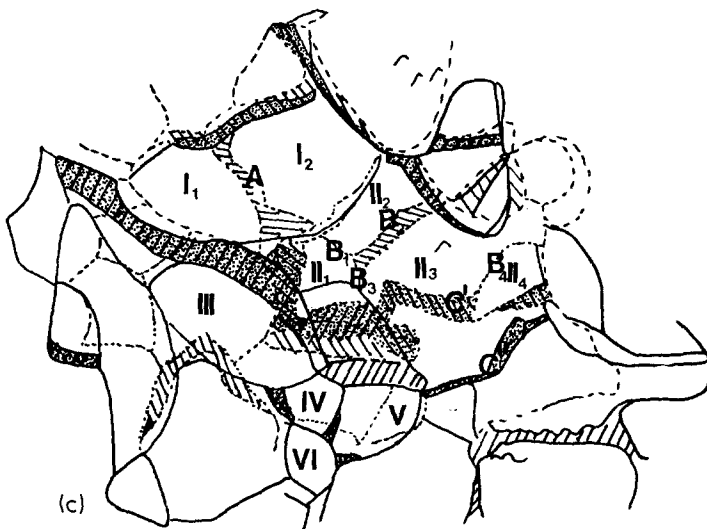
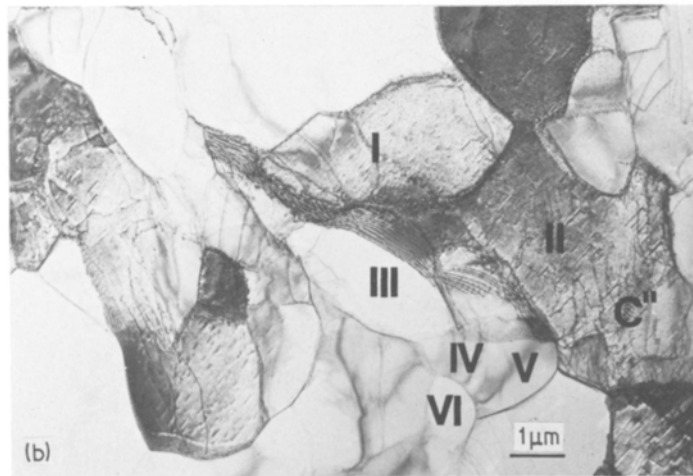
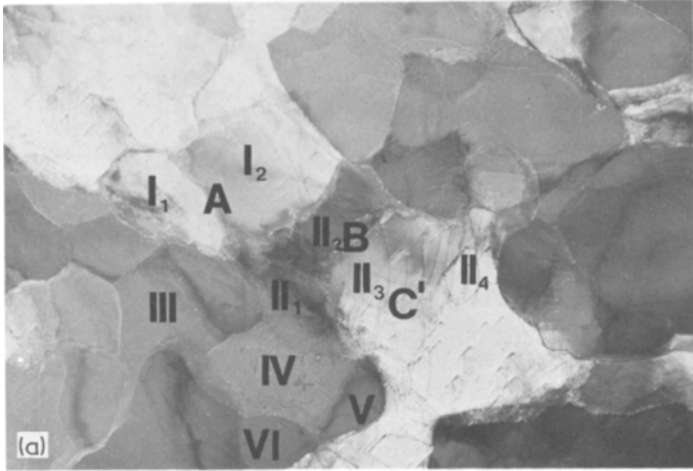


Figure 8 Specimen (a) before and (b) after annealing in the high voltage electron microscope. Simultaneous growth due to sub-boundary migration and sub-grain coalescence is illustrated. The positions of the sub-boundaries in (a) and (b) are superimposed in (c). The notation is explained in the text. - - - before annealing; — after annealing.

dislocations move from boundary A to B. At the same time as the dissolution takes place, the dislocation density in the subgrain interiors is decreasing, illustrating the close connection between the extraction of boundary dislocations and the recovery. Both annihilation and absorption at the boundaries contribute to the recovery. Thus, for example, the two dislocations marked c are absorbed by the boundary B.

In Fig. 7 another sequence illustrates the extraction of a dislocation "a" from the boundary A. The segment of the dislocation lying in the boundary cannot be seen on the micrographs.

However, from the video-tape it can be confirmed that the dislocation is extracted from the boundary.

Specimens have also been annealed *in situ* at higher temperatures of the order of 300°C. It is possible to study subgrain growth at higher temperature in thin foils than in bulk material, because the recrystallization is strongly retarded by the presence of the foil surfaces [9]. An example is given in Fig. 8. The substructure before and after the annealing is shown in Figs. 8a and b. To simplify the comparison between the two micrographs, the positions of the boundaries have

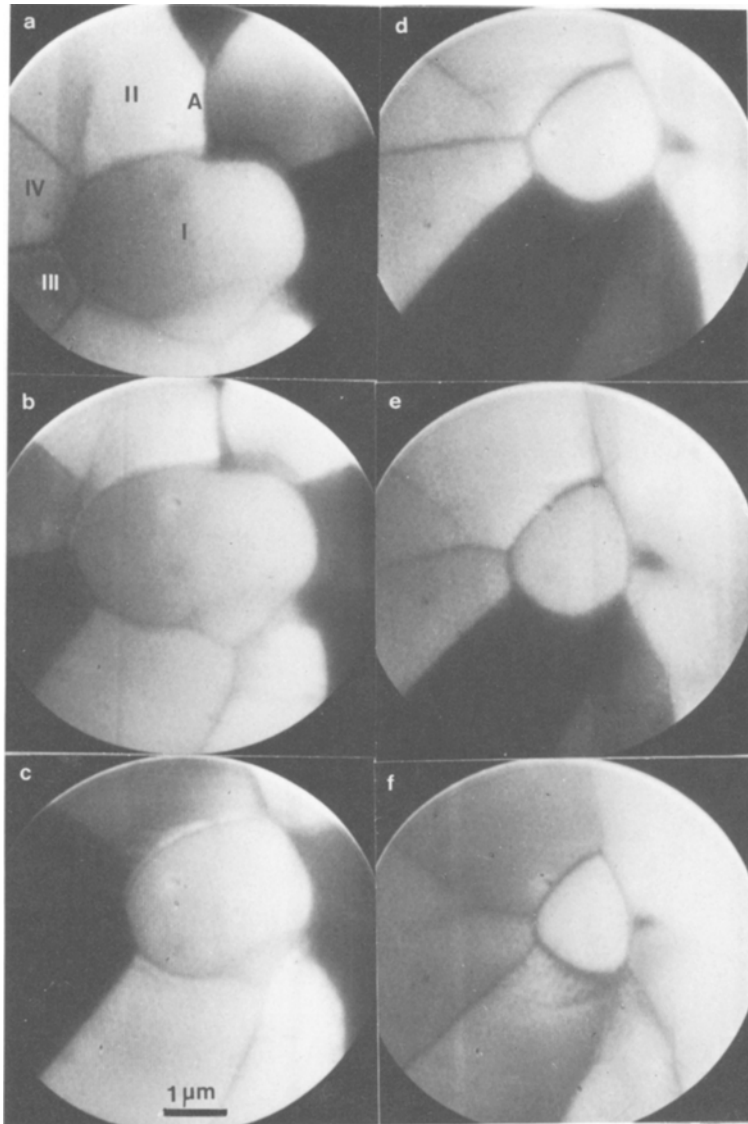


Figure 9 Growth by sub-boundary migration. The subgrain I is gradually consumed by its neighbours. The shrinkage of I is followed by rearrangement of the neighbouring grains. Thus II and III are in contact at the beginning but not at the end of the sequence, while for I and IV the reverse occurs.

been superimposed in Fig. 8c. A number of coalescence events is seen. The boundary A has disappeared in Fig. 8b causing the coalescence of the subgrain I_1 and I_2 to I. The subgrain II consisted of no less than four subgrains II_1 , II_2 , II_3 and II_4 in Fig. 8a. The coalescence has taken place by the removal of the walls B_1 , B_2 , B_3 and B_4 . The size of II has increased further by the migration of C from C' to C'' . Fairly complex rearrangement of subgrain boundaries has occurred in several instances. Examples are the subgrains III, IV and V. The curvature of many boundaries is reversed between Fig. 8a and b. The reversal may take place very rapidly, which makes it difficult to use the curvature to predict the direction of migration of a boundary. If this could be done,

one would expect the walls to migrate towards their centre of curvature. One example of this type of behaviour is the small subgrain VI which has decreased in size.

Growth by sub-boundary migration is shown in Fig. 9. The sequence illustrates how the subgrain I is gradually consumed by its neighbours. The shrinkage of I occurs in much the same way as the shrinkage of a small grain in conventional grain growth. Hence, the boundaries are migrating towards their centre of curvature. For several boundaries the centre of curvature is changing from one side to the other even during this short sequence, as for the boundary A. Another phenomenon frequently occurring during conventional grain growth appears in this sequence.

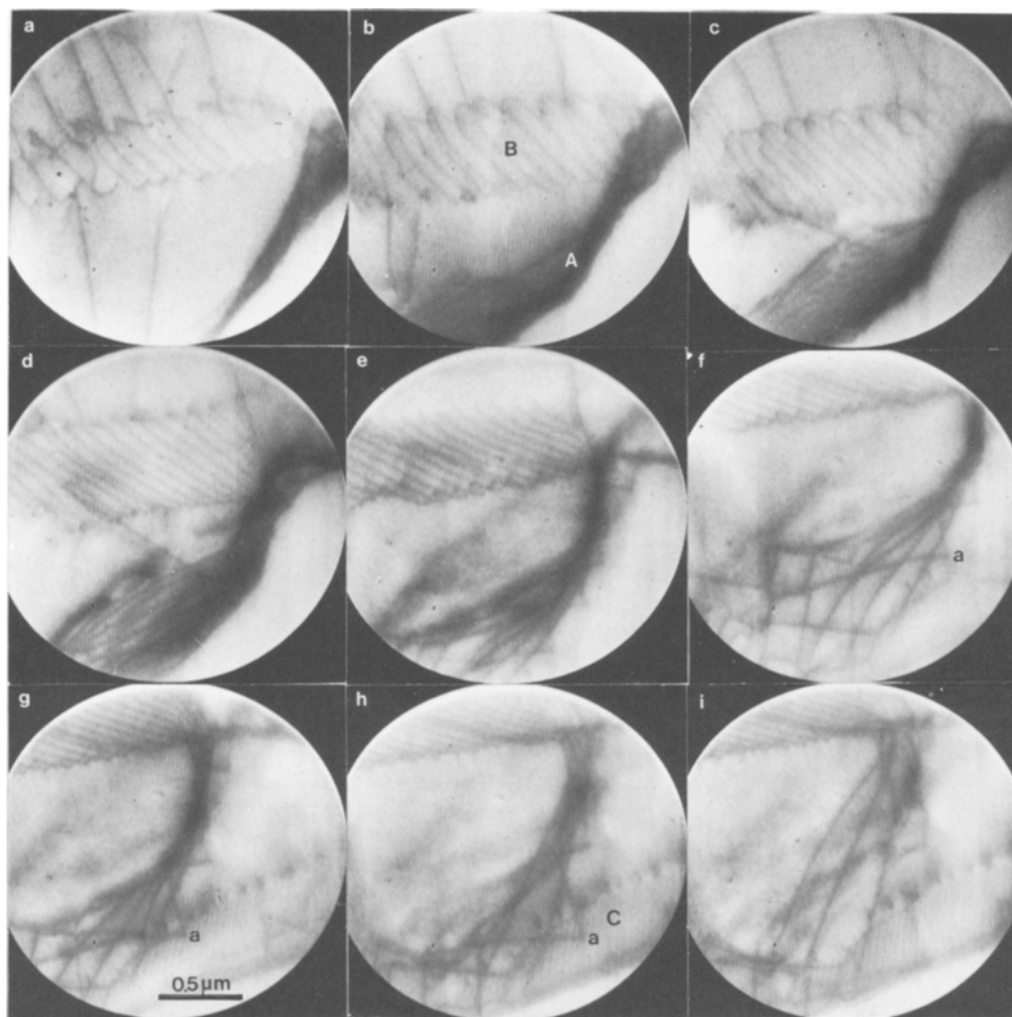


Figure 10 The dissolution of a migrating boundary (marked A). The dissolution occurs in two ways, by migration of dislocations along the boundary towards the boundary B, which thickens during this process, and by extraction of dislocations, for example "a", which is absorbed by the boundary C.

Grains which are not in contact in the beginning of the sequence like II and III, are neighbours at the end, while on the other hand the subgrains I and IV have lost contact.

The dissolution of a migrating boundary is shown in Fig. 10. The boundary under consideration is marked A. Figs. 10a to c illustrate how A migrates towards the boundary B, before the distances between A and B increases again. The start of the dissolution is clearly evident from Fig. 10d and onwards. The dissolution occurs in two ways. Boundary dislocations are being pulled out towards C. From the tape it can be seen how one dislocation after the other leave B entering boundary C instead. One example is "a". Some dislocations are also moving along the boundary towards A and gradually absorbed by this boundary. It is also apparent from the sequence of micrographs that the density of dislocations in B is successively increasing.

It can be concluded that the mechanisms for growth depend on the annealing temperature. At the lower temperatures examined no boundary migration takes place, and all growth is the result of the dissolution of boundaries. At the higher temperatures extensive boundary migration occurs as well as dissolution of boundaries. Fujita [10] in his *in situ* HVEM experiments on aluminium did not find any boundary migration at 150°C, but he frequently observed migration above 300°C in agreement with the present studies.

5. Comparison with the model

In the discussion above only evidence from growth by extraction of dislocations from the boundaries has been found in the temperature interval 100 to 200°C, where the growth rate was measured for pure aluminium. The theoretical model derived for this mechanism in [2] yields the following growth rate,

$$\frac{dD}{dt} = M\tau\phi\rho h/\mu, \quad (8)$$

where ϕ is the inverse of the fraction of the distance traversed by climb for an extracted dislocation, ρ is the dislocation density in the subgrain interior, and h is the average distance between the dislocations in a sub-boundary. μ is a constant of about 2 to 3. The recovery occurs in two steps, one rapid and one slower, where pair annihilation and absorption at the boundaries respectively are the dominating processes [2]. Since in the present

case recovery has taken place during the cold working, and well developed sub-boundaries have been formed, the first step is assumed to be completed before the start of the annealing. Thus, the behaviour during the second step is assumed to prevail. Under these condition the growth can be described by the following implicit equation [2]

$$D - D_0 + D_1 \ln \frac{D_1 - D}{D_1 - D_0} = -\frac{\beta M \tau \phi}{D_1 (1 - \beta/3)} (t - t_0) \quad (9)$$

$$\text{where } D_1 = \frac{D^{\beta/3}}{a}$$

a being a constant related to the initial subgrain diameter, D_0 , and growth rate. β is the fraction of the total driving force acting on the dislocation. The relationship above is plotted in Fig. 3. The values of the parameters used are $D_0 = 0.71 \mu\text{m}$, $\beta = 0.5$, $a = 10^5 \text{ m}^{-5/6}$, $\phi = 10^3$ and $\tau = 10^{-9} \text{ N}$. For the dislocation mobility M the values 9.4×10^{-11} , 8.4×10^{-10} and $4.3 \times 10^{-9} \text{ m}^2 \text{ N}^{-1} \text{ sec}^{-1}$ at 100, 150 and 200°C respectively have been applied. With the aid of the expression given in Equation 5 the mobility M can be evaluated. For D_s values have been taken from [6] ($D_s^0 = 10^{-5} \text{ m}^2 \text{ sec}^{-1}$, $Q = 127 \text{ kJ mol}^{-1}$, $D_s = D_s^0 \exp(-Q/RT)$). The resulting values for M are 7.5×10^{-13} (100°C), 8.5×10^{-11} (150°C), and $3.5 \times 10^{-9} \text{ m}^2 \text{ N}^{-1} \text{ sec}^{-1}$ (200°C). The values for D_s^0 and Q are only valid down to 330°C, and the extrapolation to still lower temperatures can be expected to underestimate D_s because of a too large activation energy. In fact the activation energy for the M values used in Fig. 3 is 56 kJ mol^{-1} . This activation energy is very close to that observed for vacancy migration which might indicate the presence of a supersaturation of vacancies. Such a supersaturation, which is not entirely unexpected considering the large reduction used in the deformation, would also explain the enhancement of the mobility values compared to the theoretical ones. The high value means that the extracted dislocations only climb over distances which are short compared to the subgrain diameter, when crossing the subgrains at these temperatures. Although it is not explicitly taken into account, one can expect that ϕ increases with decreasing temperature.

Using the same mobilities the contribution from the collective migration of dislocations can

be evaluated. It is found that it increases approximately linearly with time to a value which is less than $0.05\ \mu\text{m}$ for the longest times shown in Fig. 3. However, as the temperature increases and ϕ decreases, the contribution from the collective migration becomes more significant.

Subgrain grain growth in pure aluminium has been measured at 200, 300, 350 and 400°C by Beck *et al.* [11]. The same amount of cold reduction was used as in the present experiments. Beck *et al.* [11] claim a purity in their material which is even higher than in the present investigation. It is highly unlikely that this is really the case for two reasons. Firstly, our material is completely recrystallized after only a few minutes at 300°C and above. Secondly, no measureable growth was detected at 200°C by Beck *et al.* The operating mechanisms for the growth observed at 300, 350, and 400°C cannot be judged with certainty. However, two facts suggest that collective migration of boundary dislocations is the main process: no limiting subgrain size was obtained, and the dislocation density in two micrographs presented appears to be low.

If the data by Beck *et al.* [11] are plotted in a diagram where D^2 is given as a function of time, one finds that the K value, i.e. the slope of the curves, decreases as a function of time. This is probably an indication of the presence of a back-stress due to impurities as was discussed in detail in [1]. The initial slopes are then closer to the theoretical values than those obtained later during growth. The theoretical values for $K(= 11M\tau_s)$ are 5.9×10^{-15} (300°C), 4.6×10^{-14} (350°C), and $2.7 \times 10^{-13}\ \text{m}^2\ \text{sec}^{-1}$ (400°C). These should be compared to the initial slopes obtained experimentally: 1.5×10^{-15} (300°C), 8.0×10^{-15} (350°C), and $5.8 \times 10^{-14}\ \text{m}^2\ \text{sec}^{-1}$ (400°C). The measured values are only larger by a factor of about five. Taking into account that the growth is probably influenced by the presence of the back-stress also in the initial stages of growth, this must be considered to be reasonable agreement.

6. Conclusions

Experimental findings for Al–1%Mn and pure Al have been compared to mechanisms proposed for subgrain growth. From the observed dislocation structure it can be concluded that different mechanisms are operating in different cases. For Al–1%Mn collective migration of boundary dislocations is the dominating mechanism. For the

observations made in the present investigation on pure Al at 100 to 200°C , the growth occurs by the dissolution of boundaries through the extraction of boundary dislocations. A high purity material was used, and it was not possible to observe growth at 250°C and above, because the material recrystallized rapidly at such temperatures. However, Beck *et al.* [11] have measured growth in aluminium with a different impurity content at 300, 350 and 400°C . Their observations suggest that collective migration of boundary dislocations is the dominating mechanism in this case. Thus a change in mechanism occurs, when going from the temperature interval 100 to 200°C to 300 to 400°C .

The measured subgrain growth rates for Al–1%Mn and Al have been compared to the models proposed for the operating mechanisms [1, 2]. It has been found that these models are consistent with the growth rates observed.

The subgrain growth rate varies substantially as a function of temperature. However, the range of subgrain sizes observed is rather limited. The reason is interference due to recrystallization. Attempts to use longer times to obtain larger subgrain sizes have been unsuccessful. After reaching a certain average subgrain diameter, recrystallization occurs. This is consistent with a model for nucleation of recrystallization [12] which says that a critical subgrain size is required, before the recrystallization can start. It is of course sufficient that the largest subgrain has reached the critical size, the average size may still be smaller.

Acknowledgements

Financial support from the Swedish Board for Technical Development is gratefully acknowledged.

References

1. R. SANDSTRÖM, *Acta Met.* **25** (1977) 905.
2. *Idem, ibid* **25** (1977) 897.
3. J. C. M. LI, *J. Appl. Phys.* **33** (1962) 2958.
4. R. SANDSTRÖM, I. GROZA and B. LEHTINEN, Proc. Microscopie électronique a haute tension, Quatrième Congrès International, Toulouse, edited by B. Jouffrey (Société Française de Microscopie Electronique, Paris, 1975) p. 269.
5. J. P. HIRTH and J. LOTHE, "Theory of dislocations" (McGraw-Hill, New York, 1968).
6. Y. ADDA and J. PHILIBERT, "La diffusion dans les solides" (Presses universitaires de France, 1966).
7. N. F. FIORE and C. L. BAUER, *Progr. Mater. Sci.* **13** (1967) 85.

8. W. HOFFMANN, *Abhandl. Braunschweig, Wiss. Ges.* **1** (1949) 83.
9. W. ROBERTS and B. LEHTINEN, *Phil. Mag.* **29** (1972) 1431.
10. H. FUJITA, *J. Phys. Soc. Japan* **26** (1969) 1437.
11. P. A. BECK, B. G. RICKETTS and A. KELLY, *Trans. AIME* **215** (1959) 949.
12. J. E. BAILEY and P. B. HIRSCH, *Proc. Roy. Soc. London A* **267** (1962) 11.

Received 30 June and accepted 7 October 1977.